Historic Automated Lung Segmentation Method: Performance on LOLA11 Data Set

Pechin Lo, Jonathan Goldin, David Oria, Ashley Banola, and Matthew Brown

UCLA Thoracic Imaging Research Group, Department of Radiology, University of California, Los Angeles, USA, `pechinlo@mednet.ucla.edu`,

Abstract. This paper presents a historical automated method (published in 1997) for segmenting lungs in chest CT scans, which we applied to the challenging dataset of LOLA11. In addition to 3D region growing and mathematical morphological operator for the lung extraction, the method also features an explicit anatomical model represented using a frame-based semantic network, and the use of fuzzy sets to incorporate anatomical variability. A blackboard architecture is used to facilitate interactions between the different components. The method was originally developed for thick sliced scans, with a slice thickness between 5 to 10 mm, and was meant to segment scans from both healthy and emphysema subjects. Despite being over 14 years old, the method performs reasonably well on the dataset of LOLA11, which contains much more abnormal scans, with a mean overlap of 96.3%.

1 Introduction

Segmentation of the lung fields is the first step for most tasks related to the analysis of the lungs in computed tomography (CT) scans, ranging from the registration of CT scans [1], segmentation of lung structures [2, 3], to quantification of lung diseases [4]. Most works related in lung segmentation in CT are region growing based, with the assumption that the lungs are objects of lower density in comparison to its surroundings, such as those presented in [5–7]. There are also more advanced methods that try to account for dense anomalies within the lungs using image registration [8, 9] or shape models [10].

The aim of this paper is to participate in the LObe and Lung Analysis 2011 (LOLA11) with our historic 14-year old method as presented in [11], which is one of the earlier automated lung segmentation methods, where it will be compared to the current state of the art methods. The method has been shown to have strong correlation with lung volumes from PFTs and be highly reproducible in the setting of emphysema treatment trials [12]. In the next section, we will give a brief description of the method used. Results from the method will be presented in Section 3, followed by the conclusion in Section 4.

2 Methodology

The overall architecture of our method centers around a blackboard, as shown in Figure 1(a), where key components interact with each other, which are the anatomical model, inference engine, and image processing routines.

In the anatomical model, the chest wall and mediastinum, central tracheo-bronchial tree, and right and left lungs are initially modeled in terms of attenuation threshold, shape, contiguity, volume, and relative position. Figure 1(b) shows the semantic network used by the anatomical model. Data within a frame are stored in the form of a series of "slot" as shown in the example for the trachea in Fig 1(c), which gives the volume of the trachea and its distance from the medial axis as fuzzy sets. Note that the value for the various parameters used in the model were determined empirically based on CT scans from healthy and emphysema patients.

The image segmentation is performed by first applying the thresholds, as indicated in Fig 1(b), on the CT scan. Connected component analysis using a 6 connected neighborhood is then applied on the resulting binary image to extract individual disconnected regions or image primitives. These image primitives are "candidates" to be matched with the anatomical model. It is possible that the anterior junction line separating the right and left lungs can be very thin. Owing to volume averaging, the CT attenuation of this soft tissue interface may be reduced such that it falls into the range considered to be lung. In order to ensure proper separation between candidates from the left and right lungs, an additional morphological opening operation using a cylindrical structural element is applied, where disconnected regions after the opening procedure are also added as candidates. To ensure more accurate separation between the disconnected components after the opening operation, the separation is refined for each slice of the joining region using dynamic programming to extract a 2D maximum cost path, where the cost of a pixel is its graylevel.

The task of the inference engine is to select the best candidate based on knowledge stored in the model, i.e., matches image structures to the model. Membership grades derived from the fuzzy sets are used by the inference engine as confidence scores to quantify how well a candidate satisfies the given constraints. The overall confidence score for a particular candidate is derived by taking the minimum of all constraint confidence scores, i.e., a fuzzylogic approach. The candidate with the highest confidence is then selected for matching to the model.

Table 1. Results of lung segmentation for the 55 scans in LOLA11.

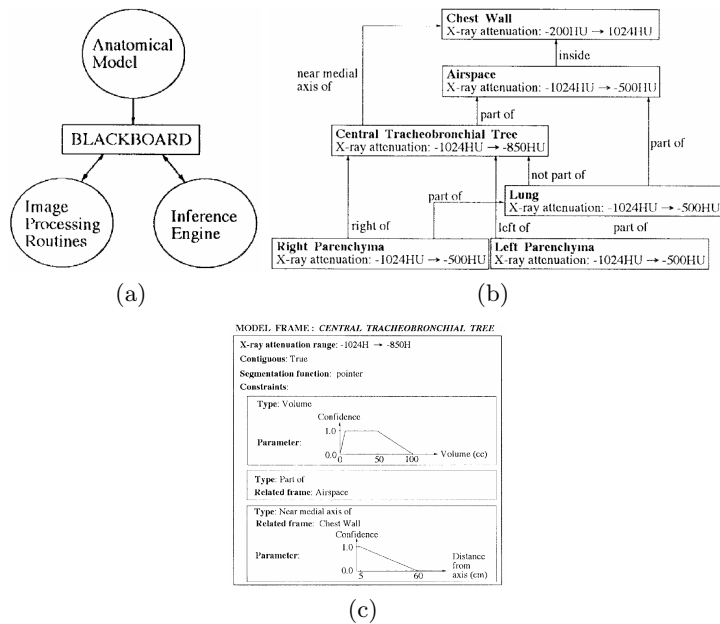|	mean	SD	min	Q1	median	Q3	max
left lung	0.965	0.101	0.247	0.976	0.986	0.991	0.995
right lung	0.962	0.134	0	0.977	0.987	0.992	0.997
score	0.963						

Fig. 1. (a) System architecture. (b) Semantic network describing thoracic anatomy related to the lungs. (c) Model frame describing the central tracheobronchial tree.

3   Results

Our method was used to segment the left and right lungs from the LOLA11 dataset, which consists of 55 CT scans that were obtained using a variety of scanners and protocols. The entire segmentation process was fully automated, without the need of any human interaction. Table 1 gives the statistics of the overlap measures between the segmented lungs of our method with the standard reference of LOLA11. The overlap measure is defined as the volume of the intersection divided by the volume of the union of the segmented lungs and the standard references. In order to account for subjectivity and inaccuracy of the manually drawn borders of the standard reference, a slack border within 2 mm of a manually drawn border is defined, where voxels within the slack borders are excluded from the evaluation. Average execution speed of our method was around 1 minute per case on a 2.34 GHz PC.

4   Conclusion

We have applied a historical automated lung segmentation method to the challenging dataset of LOLA11. Despite the fact that the method was originally developed for thick sliced scans and was meant for segmenting scans from both

healthy and emphysema subjects, reasonably good results were achieved on the dataset of LOLA11, which contains much more abnormal scans in terms of lung opacity and structural deformations, with a mean overlap of 96.3%.

References

1. Wu, Z., Rietzel, E., Boldea, V., Sarrut, D., Sharp, G.C.: Evaluation of deformable registration of patient lung 4DCT with subanatomical region segmentations. Medical Physics **35**(2) (Feb 2008) 775–781
2. Ochs, R.A., Goldin, J.G., Abtin, F., Kim, H.J., Brown, K., Batra, P., Roback, D., McNitt-Gray, M.F., Brown, M.S.: Automated classification of lung bronchovascular anatomy in CT using AdaBoost. Medical Image Analysis **11**(3) (June 2007) 315–324
3. van Rikxoort, E.M., van Ginneken, B.: A pattern recognition approach to enhancing structures in 3D CT data. In Joseph M. Reinhardt, J.P.W.P., ed.: Medical Imaging 2006: Image Processing. Volume 6144., SPIE (March 2006) 569–576
4. Dirksen, A., Piitulainen, E., Parr, D.G., Deng, C., Wencker, M., Shaker, S.B., Stockley, R.A.: Exploring the role of CT densitometry: A randomised study of augmentation therapy in Alpha1-antitrypsin deficiency. European Respiratory Journal **33**(6) (Jun 2009) 1345–1353
5. Hu, S., Hoffman, E., Reinhardt, J.: Automatic lung segmentation for accurate quantitation of volumetric X-ray CT images. IEEE Transactions on Medical Imaging **20**(6) (June 2001) 490–498
6. Weinheimer, O., Achenbach, T., Buschsiewke, C., Heussel, C.P., Uthmann, T., Kauczor, H.U.: Quantification and characterization of pulmonary emphysema in multislice-CT. In: International Symposium on Medical Data Analysis (ISMDA). (2003) 75–82
7. Sun, X., Zhang, H., Duan, H.: 3D computerized segmentation of lung volume with computed tomography. Academic Radiology **13**(6) (June 2006) 670–677
8. Sluimer, I., Prokop, M., van Ginneken, B.: Toward automated segmentation of the pathological lung in CT. IEEE Transactions on Medical Imaging **24**(8) (Aug. 2005) 1025–1038
9. van Rikxoort, E., de Hoop, B., Viergever, M., Prokop, M., van Ginneken, B.: Automatic lung segmentation from thoracic computed tomography scans using a hybrid approach with error detection. Medical Physics **36**(7) (2009) 2934–2947
10. Li, B., Reinhardt, J.: Automatic generation of object shape models and their application to tomographic image segmentation. In Sonka, M., Hanson, K., eds.: Medical Imaging 2001: Image Processing. Volume 4322., SPIE (July 2001) 311–322
11. Brown, M.S., McNitt-Gray, M.F., Mankovich, N.J., Goldin, J.G., Hiller, J., Wilson, L.S., Aberie, D.R.: Method for segmenting chest ct image data using an anatomical model: preliminary results. IEEE Transactions on Medical Imaging **16**(6) (1997) 828–839
12. Brown, M.S., Kim, H.J., Abtin, F., Costa, I.D., Pais, R., Ahmad, S., Angel, E., Ni, C., Kleerup, E.C., Gjertson, D.W., McNitt-Gray, M.F., Goldin, J.G.: Reproducibility of lung and lobar volume measurements using computed tomography. Academic Radiology **17**(3) (Mar 2010) 316–322